DOI: 10.38061/idunas.843533

IDUNAS | NATURAL & APPLIED SCIENCES JOURNAL | 2021 Vol. 4 No. 2 (53-60)

Static Compression and Dynamic Sliding Conditions of 2D Trapezoid Square and Circle Contact Surface Shapes

Research Article

Mustafa Murat Yavuz[1*]

[1]Department of Mechanical Engineering, İzmir Democracy University, İzmir, Turkey.

Author E-mails
murat.yavuz@idu.edu.tr
*Correspondance to: Mustafa Murat Yavuz, Department of Mechanical Engineering, İzmir Democracy University, İzmir, Turkey.
DOI: 10.38061/idunas.843533

Received: 19.12.2020; Accepted: 17.02.2021

Abstract

In addition to the commonly encountered force-body interaction problems, deformable body problems are frequently encountered in engineering applications and examination conditions are more complex. The friction force and contact pressure formed between the surfaces have dominant effects and mostly studies are investigated considering static and quasi-static conditions. However, considering the elastic/elasto-plastic deformation and dynamic conditions, the geometric surface shape is important. In this study, using the finite element analysis method, the pressure distribution of the surfaces containing square, trapezoidal and circular surface shapes on a flat surface and the dynamic deceleration condition during the surface interaction of an object with initial velocity are investigated. The material used is steel whose ground geometry does not show linear behaviour and nylon material is used for surface geometry. In order to ensure that the surface effect is dominant in the dynamic examination, a linear increasing pressure is applied on the examined part. In the results, it was determined that there was an irregularity in the stress and velocity deceleration curve. The effect of compression pressure and friction coefficient has been examined in detail and the results are discussed.
Keywords: Contact pressure, surface stress, dynamic, deformation.

1. INTRODUCTION

The deformation of the contact surfaces due to mechanical effects is an important factor for the parts. The effects on the contact surfaces vary depending on the applied pressure and the friction force between the surfaces. However, surface shapes are also important because deformation in dynamic conditions changes the contact surfaces and shape significantly. The flat contact surface is designed differently according to the conditions. Haines and Ollerton [1] studied contact stress distributions on elliptical contact surfaces considering Hertz theory. The adhesive effects caused different shear stress distribution rather than simple strip theory. Johnson et al. [2] discussed the force of adhesion and contact size effect between two spherical solid surfaces. Surface energy concept was considered with rubber and gelatine spheres. In literature, contact surface shapes [3] were optimized for better and more uniform contact

pressure distribution. Senouci et al. [4] investigated wear behaviour of graphite-copper sliding contact. Anisotropic graphite causes incompatibility between mechanical and tribological behaviour. Kimura et al. [5] investigated wear and fatigue of contact rollers in which microslip condition had a dominant effect. Herskovits et al. [6] prepared a bilevel program for shape optimization of elastic solids contact problems. Both shape optimization and nonlinear contact analysis solutions were carried out simultaneously. Li et al. [7] studied on shape optimization for contact problems including combined loadings. Goryacheva et al. [8] considered partial slip conditions in fretting and prepared an analytical model. Archard's wear law was used for wear development and they calculated contact pressure and shear stress, contact width, gap and slip functions using stepwise formulation. Brake pads including hatched shapes [9] were considered that increases fade resistance. Araujo and Nowell [10] investigated effect of contact stress variation on fretting fatigue and demonstrated contact size effect in fretting fatigue life. Triangle, trapezoid, parallelogram and rectangular block shapes [11] were investigated for stress reduction in tilt tests. Jiang et al. [12] studied 3D elasto-plastic stress analysis of contact rollers with kinematic hardening. Shear tractions had a dominant effect on residual stresses and strains. Wen et al. [13] modelled wheel/rail contact-impact behaviour with kinematic hardening. During dynamic analysis, peak force effect was observed 2.6 times greater than static results. Gerlici and Lack [14] investigated influence of contact geometry and calculated surface stress distributions of wheel-rail interaction. Rovira et al. [15] and Dirks and Enblom [16] studied on contact and wear interaction of wheel-rail. Contact interface of adhesive binding [17] was investigated for optimal surface shapes. Contact behaviour of complex surface shapes [18] were investigated for punches.

In this study, using the finite element method, contact levels with different surface shapes in dynamic conditions have been investigated. The study is made in 2D. Properties of different compression pressures were used, and the effect of the friction coefficient was examined separately. Results are compared as Von-Mises stress.

2. MODELS AND METHOD

Three different surface shapes used in the study were shown in Fig. 1. Surface shapes formed in trapezoid, circular and rectangular shapes were studied on a flat plane with the initial velocity in the horizontal right direction. Initial velocity is 5 m/s horizontally. All geometric properties in 2D are shown in the Fig. 1. Different shaped parts contacting the surface as material are selected as nylon and other parts are modelled to include steel material properties. While the moving contact surface modelled in different geometries contains nylon properties, other parts are modelled to contain steel material properties. 0.1 MPa surface pressure applied to the shoe geometry to see the friction effect more clearly. Solution time was chosen as 1.4 milliseconds (ms).. Friction coefficient is used as 0.3 as default. Fancelle et al. [19] used Augmented-Lagrangian algorithm for contact modelling and interior-point method for shape optimization in 2D frictionless finite element solution. Similarly, Augmented-Lagrange contact algorithm was used in this analysis.

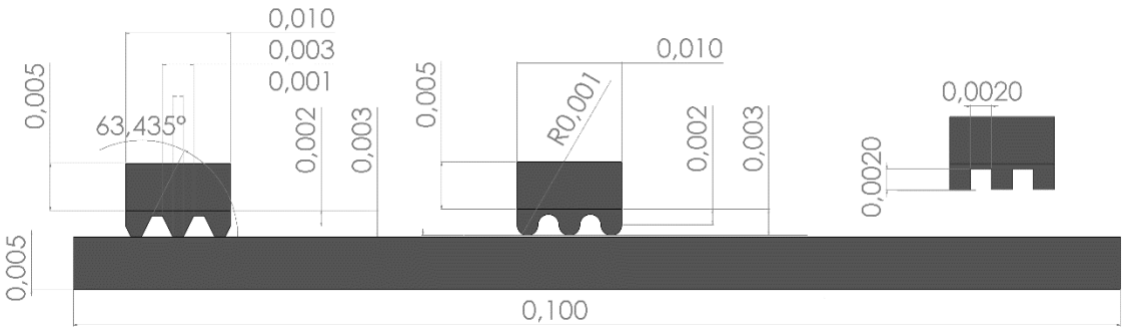

Figure 1. Models of trapezoid, circle and square contact surface shapes.

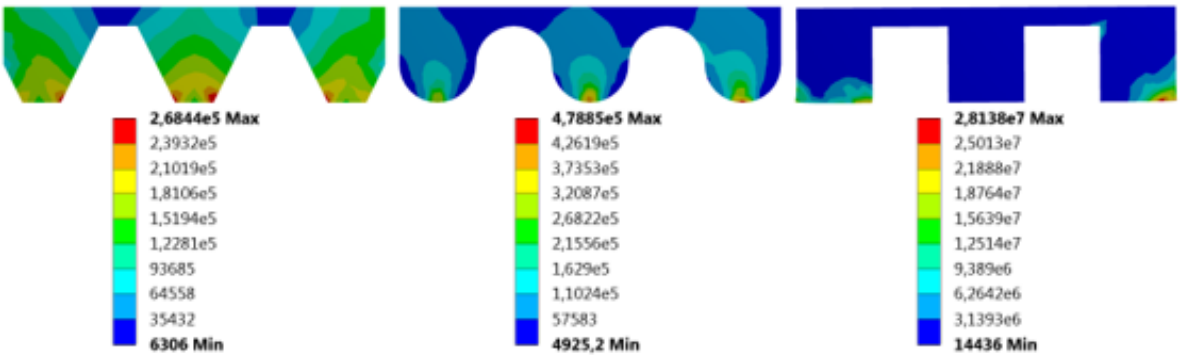

Figure 2. Von-Mises stresses of trapezoid, circle and square contact surface shapes.

The Von-Mises stresses created by different contact geometries were shown in Fig. 2. Considering the results, the stress density formed at the end corners of the trapezoid geometry. The intensity of this stress was mostly at the inner corners of the 3 pieces. In the round tip contact geometry, the stress distribution occurred as a result of full contact. In the rounded contact geometry, the stress distribution occurred at the full contact end points. The stress value was approximately 2.6 times higher than applied pressure which was similar results of the Wen et al. [13] study Considering the stress results in the square shaped model, it was seen that the stress reached the highest value at the corner end in the direction of movement and a stress jump was determined. The low stress in the square geometry in the middle section indicated a non-contact condition. At this point the stress value was 100 times higher than the results of the trapezoid shape. Fig. 3 results showed the coefficient of friction results for round geometries. Stress distributions were formed in the same structure with different friction coefficients. However, with the increasing friction coefficient, the stress values first decreased and then remained constant. Fig. 4 results showed the effect of applied contact pressure. Considering the results, increasing the applied contact pressure allowed to increase stress values to very high. In the last case, the stress value remained approximately the same.

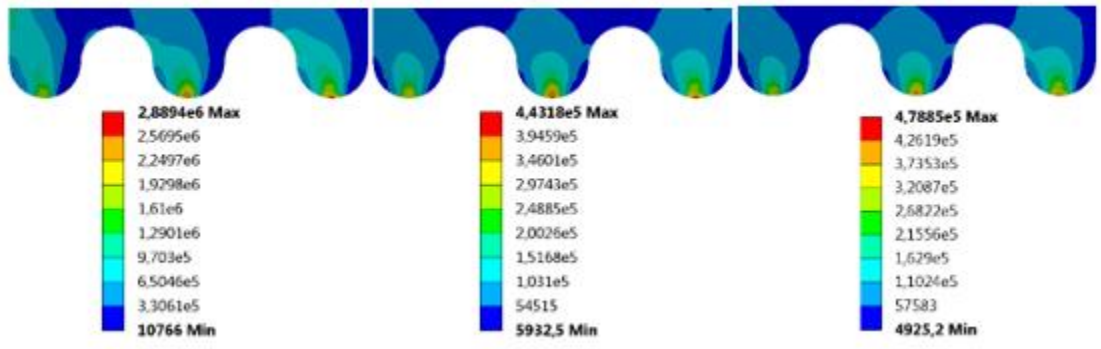

Figure 3. Von-Mises stresses of circle contact surface shape under 0.2, 0.25, 0.3 friction coefficient.

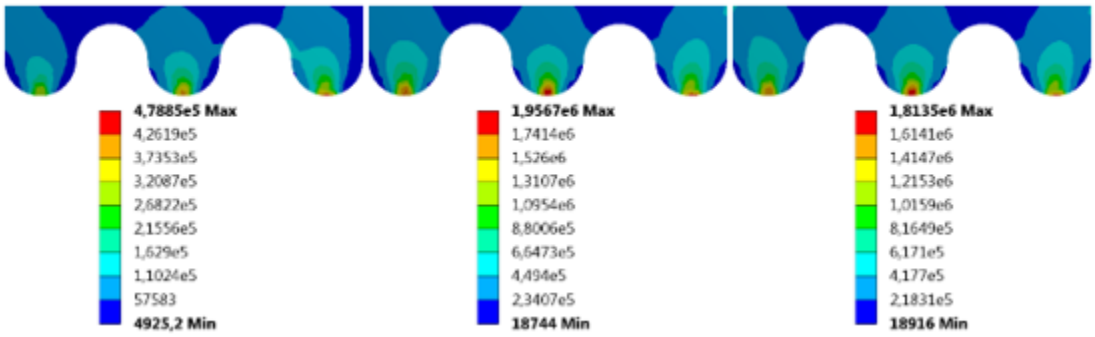

Figure 4. Von-Mises stresses of circle contact surface shape under 0.1, 0.2 and 0.3 MPa compression pressure.

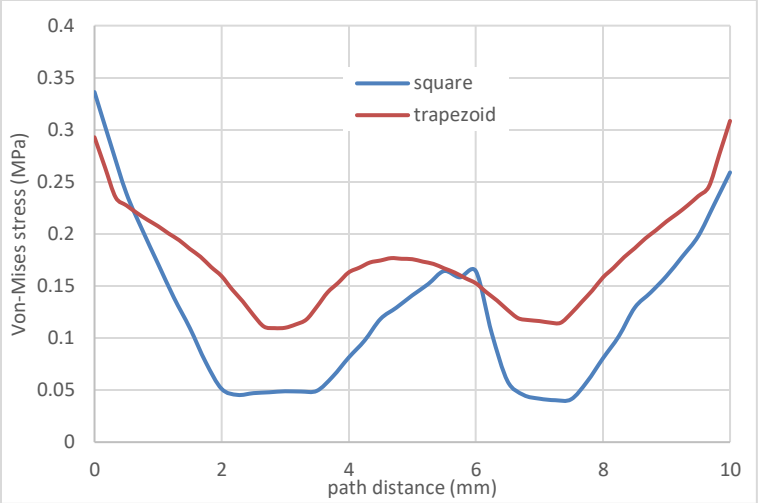

Figure 5. Von-Mises stresses of square and trapezoid contact surface shape under static compression.

In Fig. 5, the stress distribution on the line 1 of the body with square and rectangular contact surfaces was shown in the graph. As a result of the examination, the stresses were higher at the corner ends, at the middle level in the middle and at the lowest level in the partition lines. The shape consists of 3 parts and the structure of the space between them caused this distribution.

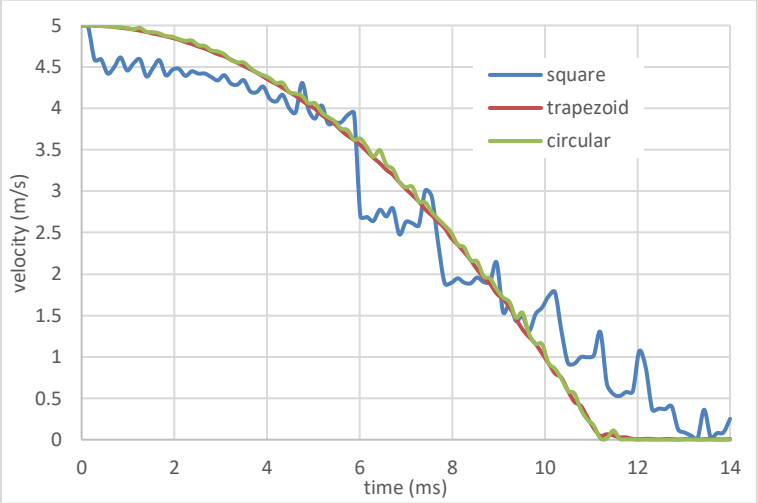

Figure 6. Velocity of trapezoid, circle and square contact surface shapes under time.

In Fig. 6, the deceleration graph of the contact surfaces with different geometric structures according to time was shown. All parts stopped at the time of 14 ms. This solution was implemented for 0.1 MPa and 0.3 friction coefficient. While the trapezoid and circular cross-section exhibited the same smooth profile, the square geometry had a very wavy structure. The non-contact situation was available in the square geometry solution. In Fig. 7, the effect of different friction coefficients was shown. In the solution using circular cross section and 0.1 MPa, a faster deceleration was achieved as a result of the increased friction coefficient. In the solution where the friction coefficient was 0.2, the part, which can stop in 14 ms, could stop in 11.6 ms when the coefficient was increased to 0.3.

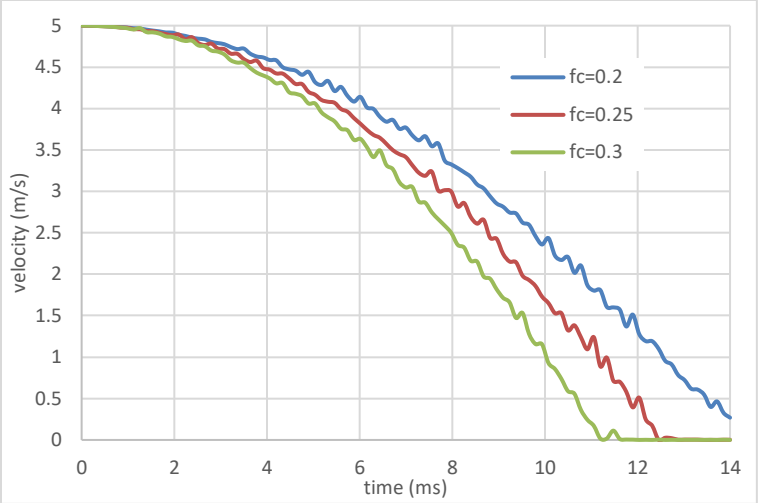

Figure 7. Velocity of circle contact surface shape under 0.2, 0.25, 0.3 friction coefficient under time.

In Fig. 8, the applied contact pressure effect was shown for the deceleration case. Stopping occurred at 11.6 ms at 0.1 MPa applied contact pressure, while at 0.2 MPa in 8 ms and at 0.3 MPa in 6.5 ms. In Fig. 9, the stress plot of all brake surfaces versus time was given. Accordingly, the square geometry used exhibited a very high stress profile. The irregular distribution was due to the regional interruption of the contact over time. Contact was maintained in the circle and trapezoid section, and the braking effect was dominant between 9 ms and 11 ms.

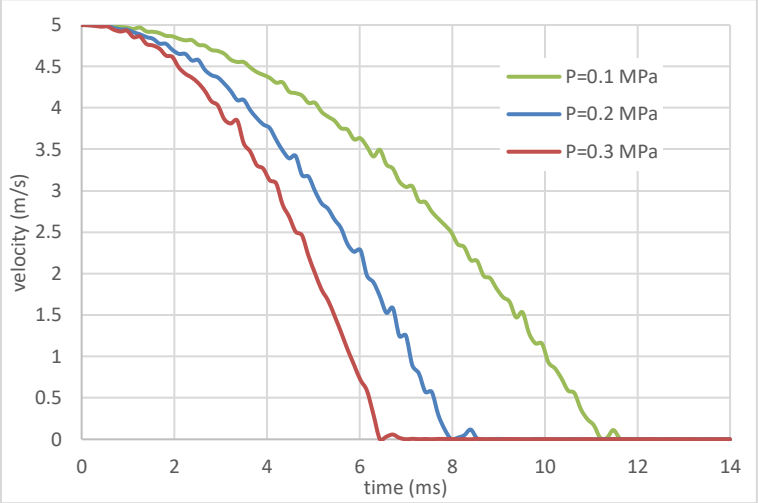

Figure 8. Velocity of circle contact surface shape under 0.1, 0.2 and 0.3 MPa compression pressure under time.

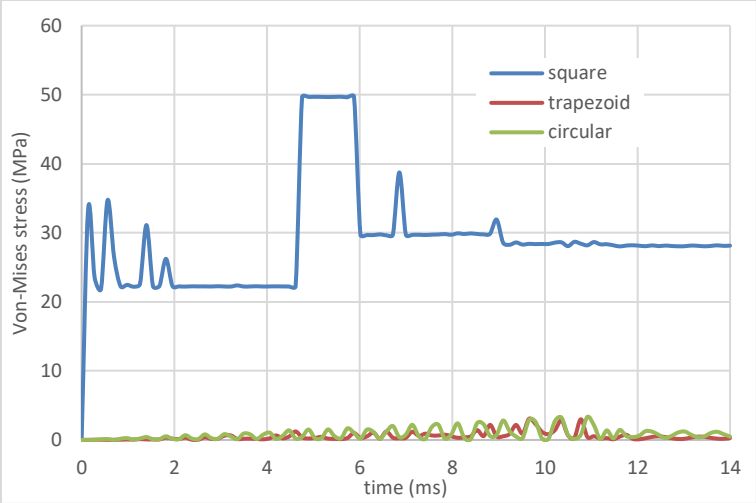

Figure 9. Von-Mises stresses of trapezoid, circle and square contact surface shapes under time

The friction coefficient effect was shown in Fig. 10 for point 1. The wave distribution that was formed as a result of dynamic effects occurred at an amplitude that increases up to 11.5 ms, which was the stopping time of objects. The highest stress amplitude appeared to be within the 0.25 friction coefficient. An instantaneous stress drop was observed in 11.5 ms at 0.2 friction coefficient, but the amplitude continued at high levels in later times. This was the case for the object did not stand still. The applied contact pressure effect was shown in Fig. 11. With the increase in pressure, the increase in amplitude showed a proportional increase. The amplitude of 0.3 MPa decreased in 6.5 ms, as it enabled the objects to stop in a shorter time with increasing contact pressure. The same has been true for other pressure results. A lower stretch amplitude continued after the decrease in amplitude.

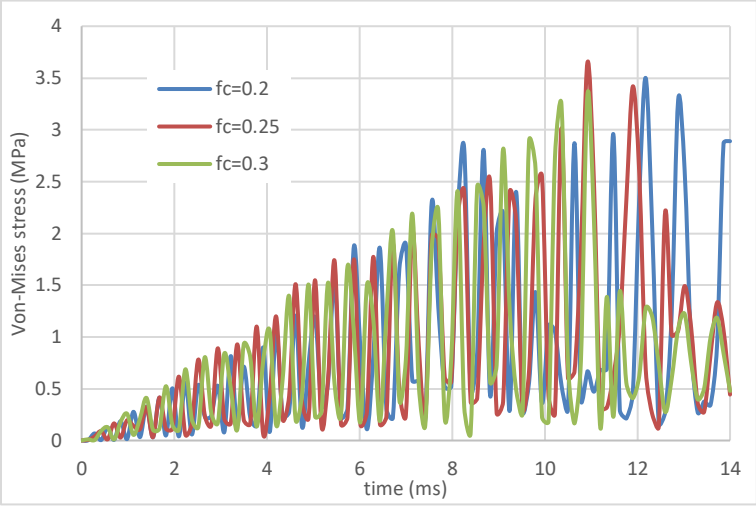

Figure 10. Von-Mises stresses of circle contact surface shape under 0.2, 0.25, 0.3 friction coefficient under time

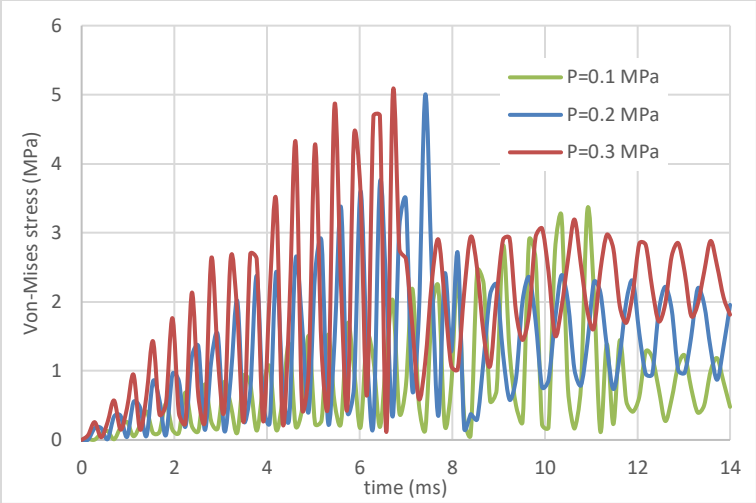

Figure 11. Von-Mises stresses of circle contact surface shape under 0.1, 0.2 and 0.3 MPa compression pressure under time

3. CONCLUSION

Trapezoid, square and circle contact surface shapes are considered for static compression and dynamic sliding conditions. A default 2D case study is applied with 0.1 MPa braking pressure, 0.3 friction coefficient and 5 m/s initial velocity. The friction coefficient and braking pressure was changed. It was observed that;

- Inner corners of trapezoid shape have the highest stress locations, but they are formed at contact points in rounded (circular) shape.
- A non-contact condition was observed in square shape.
- The increased friction coefficient causes to decrease stress values at first than causes to remain constant.
- A non-linear stress increment has been observed when increasing the applied contact pressure.

4. REFERENCES

1. Haines, D.J., and Ollerton, E. (1963). Contact stress distributions of elliptical contact surfaces subjected to radial and tangential forces. Proc Instn Mech Engrs, 177(4).

2. Johnson, K.L., Kendall, K., Roberts, A.D. (1971). Surface energy and the contact of elastic. Proc. R. Soc. Lond. A., 324, 301-313.

3. Páczelt, I., Mróz, Z. (2005). On optimal contact shapes generated by wear, Numerical Methods in Engineering, 63(9), 1250-1287.

4. Senouci, A., Frene, J., Zaidi, H. (1999). Wear mechanism in graphite–copper electrical sliding contact. Wear, 225–229, 949–953.

5. Kimura, Y., Sekizawa, M., Nitanai, A. (2002). Wear and fatigue in rolling contact. Wear, 253, 9–16.

6. Herskovits, J., Leontiev, A., Dias, G., Santos, G. (2000). Contact shape optimization: a bilevel programming approach. Struct Multidisc Optim, 20, 214–221.

7. Li, W., Li, Q., Steven, G.P., Xie, Y.M. (2005). An evolutionary shape optimization for elastic contact problems subject to multiple load cases. Comput. Methods Appl. Mech. Engrg., 194, 3394–3415.

8. Goryacheva, I.G., Rajeev, P.T., Farris, T.N. (2001). Wear in partial slip contact. Transactions of the ASME, 123, 848-856.

9. Albatlan, S. A. A. (2013). Study effect of pads shapes on temperature distribution for disc brake contact surface. International Journal of Engineering Research and Development, 8(9), 62-67.

10. Araujo, J.A., Nowell, D. (2002). The effect of rapidly varying contact stress fields on fretting fatigue. International Journal of Fatigue, 24, 763–775.

11. Kim, D. H.; Gratchev, I. Hein, M. Balasubramaniam, A. (2016). The application of normal stress reduction function in tilt tests for different block shapes. Rock Mechanics and Rock Engineering, 49, 3041–3054.

12. Jiang, Y., Xu, B., Sehitoglu, H. (2002). Three-dimensional elastic-plastic stress analysis of rolling contact. Journal of Tribology, 124, 699-708.

13. Wen, Z., Jin, X., Zhang, W. (2005). Contact-impact stress analysis of rail joint region using the dynamic finite element method. Wear, 258, 1301–1309.

14. Gerlici, J., Lack, T. (2010). Contact geometry influence on the rail / wheel surface stress distribution. Procedia Engineering, 2, 2249-2257.

15. Rovira, A., Roda, A., Marshall, M.B., Brunskill, H., Lewis, R. (2011). Experimental and numerical modelling of wheel–rail contact and wear. Wear, 271, 911– 924.

16. Dirks, B., Enblom, R. (2011). Prediction model for wheel profile wear and rolling contact fatigue. Wear, 271, 210–217.

17. Yao, H. Gao, H. (2016). Optimal shapes for adhesive binding between two elastic bodies. Journal of Colloid and Interface Science, 298(2), 564-572.

18. Kazakov, K. E. (2018). Contact between a regular system of punches and a layered foundation with consideration of complex surface shapes. AIP Conference Proceedings, 2053(1), 040041.

19. Fancelle, E.A., Haslinger, J., Feijoo, R.A. (1995). Numerical comparison between two cost functions in contact shape optimization. Structural Optimization 9, 57-68.